# Synthesis, structure and electrochemical characterization of the isopolytungstate (W4O16) held by MnII anchors within a superlacunary crown heteropolyanion {P8W48}

Article (Accepted Version)

Dalton Transactions

An international journal of inorganic chemistry

Accepted Manuscript






ROYAL SOCIETY OF CHEMISTRY

rsc.li/dalton

View Article Online
DOI: 10.1039/C9DT02478F

ARTICLE

# Synthesis, Structure and Electrochemical Characterization of the Isopolytungstate ($W_4O_{16}$) held by $Mn^{II}$ Anchors within a Superlacunary Crown Heteropolyanion $\{P_8W_{48}\}$

Received 00th January 20xx,
Accepted 00th January 20xx

DOI: 10.1039/x0xx00000x

**Masooma Ibrahim[a*], Israël M. Mbomekallé[b], Pedro de Oliveira[b], George E. Kostakis[c], Christopher E. Anson[d]**

An isopolyanion $\{W_4O_{16}\}$ within archetypal $\{P_8W_{48}\}$ heteropolyanion assembly $[(P_8W_{48}O_{184})(W_4O_{16})K_{10}Li_4Mn_{10}Na(H_2O)_{50}Cl_2]^{15-}$ **($Mn_{10}W_4$-$P_8W_{48}$)** has been synthesized by the reaction of the cyclic superlacunary anion $[H_7P_8W_{48}O_{184}]^{33-}$ and $Mn(ClO_4)_2.6H_2O$ in I M LiCl soultion medium at pH 8. The isolated compound has been characterized by single crystal X-ray crystallography, powder X-ray diffraction (PXRD), Fourier-transform infrared (FTIR) spectroscopy, elemental analysis and thermogravimetric analysis. Electrochemical studies were also performed on **$Mn_{10}W_4$-$P_8W_{48}$** confirmed the presence of Mn centres bonded to the tunsgtic framework. The novel polyanion $[(P_8W_{48}O_{184})(W_4O_{16})K_{10}Li_4Mn_{10}Na(H_2O)_{50}Cl_2]^{15-}$ is the first example of macrocyclic complex where an isopolyanion $(W_4O_{16})^{8-}$ is embedded within in the inner cavity of the $\{P_8W_{48}\}$ and is placed in position by six $Mn^{II}$ cations as anchors. Whereas, the exocyclic coordination of the four $Mn^{II}$ atoms to $\{P_8W_{48}\}$ yields extended structure by linking neighbouring polyanions through {W–O–Mn–O–W} bridges. Further, the polyanion **$Mn_{10}W_4$-$P_8W_{48}$** is the first derivative of $\{P_8W_{48}\}$ with six $Mn^{II}$ ions (largest) coordinated to the inner side the crown ring as anchors.

## Introduction

Polyoxometalates (POMs) are inorganic compounds that form between oxygen and early transition-metals (M = V, Nb, Ta, Mo, W) in their highest oxidation state and are being extensively studied because of their application in catalysis, molecular magnetism, biochemistry, analytical chemistry and separation science.[1–6] Lacunary POM ligands are versatile all-inorganic molecular precursors for the construction of molecule-based materials. Meanwhile, the structural varieties and functionalities of these materials could be tuned by the incorporation of different transition metal (TM) ions,[6–9] rare earth (RE) metal cations,[10–16] and mixed TM-RE metal centers [17–20] within the POM framework.

The archetypal macrocyclic phosphotungstate $[H_7P_8W_{48}O_{184}]^{33-}$ $\{P_8W_{48}\}$ was isolated in 1985 by Contant and Tezé.[21] This polyanion has a wheel-shaped structure and is composed of four identical hexalacunary $[H_2P_2W_{12}O_{48}]^{12-}$ Wells–Dawson fragments which are linked to each other via oxo-bridges resulting in a cyclic arrangement. Interestingly, Contant concluded that $\{P_8W_{48}\}$ is not reactive towards divalent or trivalent transition-metal ions. Nevertheless, Kortz's $[Cu_{20}Cl(OH)_{24}(H_2O)_{12}(P_8W_{48}O_{184})]^{25-}$ in 2005 drew attention to the fact cyclic anionic POM $\{P_8W_{48}\}$ is an excellent superlacunary "molecular container" system for the "cluster within cluster" assmblies.[22] Since then $\{P_8W_{48}\}$ was investigated widely and some other 3d-, 4d-, 4f-transition metals, and main group metal derivatives of the archetypal polyanion have been synthesized such as: $\{Cu_{20}\text{-}N_3\}$,[23] $\{Cu_{20}X$ (X=Br, I)$\}$,[24] $\{V^V_4V^{IV}_2\}$,[25] $\{Fe_{16}\}$,[26] $\{Mo_4O_4S_4W\}$,[27] $\{Mo_4O_4S_4\}$,[27] $\{Sn_8\}$,[28] $\{As_4\}$,[29] $\{TM_4$ (TM=Co, Mn, Ni, V$\}$,[30] $\{Ru_4\}$,[31] $\{Ln_2$ (Ln = La, Ce, Pr, Nd$\}$,[32] and {Se4}.[33] The As-analogue $[H_4As_8W_{48}O_{184}]^{36-}$ of the cyclic polyanion have been prepared and characterized as well.[34]

Further, $\{P_8W_{48}\}$ plays an essential role in the development of carbon-free functional inorganic framework.[35–37] An important example is $K_{18}Li_6[Mn_8(H_2O)_{48}P_8W_{48}O_{184}]\cdot 108H_2O$, exhibiting rigid cages with an approximate volume of 7.24 nm.[38] Very recently, $\{[Na(NO_3)(H_2O)]_4[Al_{16}(OH)_{24}(H_2O)_8(P_8W_{48}O_{184})]\}^{16-}$ and $[Ga_{16}(OH)_{32}(P_8W_{48}O_{184})]^{24-}$ with largest $Al^{III}$/$Ga^{III}$-oxo clusters encapsulated within the cavity of $\{P_8W_{48}\}$ have been reported, which also which exhibit a high proton conductivity.[39]

[a] Institute of Nanotechnology, Karlsruhe Institute of Technology, Hermann von-Helmholtz Platz 1, 76344 Eggenstein-Leopoldshafen, Germany. *Corresponding author- E-mail: masooma.ibrahim@kit.edu
[b] Equipe d'Electrochimie et Photo-électrochimie, Laboratoire de Chimie Physique, Université Paris-Sud, UMR 8000, CNRS-Université Paris Saclay, Orsay F-91405, France.
[c] Chemistry Department, University of Sussex, Sussex House, Falmer Brighton, BN1 9RH United Kingdom.
[d] KIT, Institute of Inorganic Chemistry, 76131 Karlsruhe, Engesserstrasse 15, D-76131, Karlsruhe, Germany.

Supramolecular assemblies through host–guest complexation have also been observed in polyoxomolybdate $\{Mo_{248}\}$ which is formed by addition of two $\{Mo_{36}\}$ units to the inner surface of the $\{Mo_{176}\}$ `wheel'.[40]

The stability of $[H_7P_8W_{48}O_{184}]^{33-}$ in aqueous solution over an unusually wide pH range (1-8) and its large anionic pocket. (diameter of around 10 Å) are highly desirable features for host–guest chemistry, where the nucleation processes in the cavity of archetype POM can allow the formation of "metal-oxo cluster within cluster" system through self-assembly mechanism. Inspired by this, we decided to investigate the chemistry of the archetypal macrocyclic phosphotungstate $\{P_8W_{48}\}$, herein we report the formation of an isopolytungstate $(W_4O_{16})$ moeity that occurs within the cavity of $\{P_8W_{48}\}$, and are held by Mn anchors within the cavity of cyclic molecule. The novel 4-$W^{VI}$-16-oxo isopolytungstate embedded polyanion $[(P_8W_{48}O_{184})(W_4O_{16})K_{10}Li_4Mn_{10}Na(H_2O)_{50}Cl_2]^{15-}$ (**$Mn_{10}W_4$-$P_8W_{48}$**) have been synthesized under normal bench conditions by the reaction of $Mn(ClO_4)_2.6H_2O$ and $K_{28}Li_5[H_7P_8W_{48}O_{184}]\cdot 92\ H_2O$ $\{P_8W_{48}\}$ in I M LiCl solution and characterized by single crystal X-ray crystallography, powder X-ray diffraction (PXRD), Fourier-transform infrared (FTIR) spectroscopy, elemental analysis and thermogravimetric analysis. Electrochemical studies were also performed on **$Mn_{10}W_4$-$P_8W_{48}$**.

## Results and discussion

### Synthesis

The title polyanion **$Mn_{10}W_4$-$P_8W_{48}$** was prepared by reaction of $Mn(ClO_4)_2.6H_2O$ with superlacunary archetypal-type polyanion $[H_7P_8W_{48}O_{184}]^{33-}$ in 1 M LiCl solution medium at pH 8 and isolated as the mixed cation salts, $K_3Li_8Mn_2[(P_8W_{48}O_{184})(W_4O_{16})K_{10}Li_4Mn_{10}Na(H_2O)_{50}Cl_2]\cdot 62H_2O$ (**KLiMn-$Mn_{10}W_4$-$P_8W_{48}$**). Synthesis of **KLiMn-$Mn_{10}W_4$-$P_8W_{48}$** is only possible with increasing the pH of the reaction mixture to ca. 10 and bringing back to pH 8. Also the use of LiCl solution as solvent and manganese(II) perchlorate seems play a crucial role in the formation of the title compound which lead to gradual increasing solubility and to release $K^+$ cations inside the cavity of the POM. The formation of $(W_4O_{16})$ occurs in situ, as a result of partial decomposition of some of the superlacunary $\{P_8W_{48}\}$ POM precursor in solution. Interestingly, addition of equivalent amount of sodium tungstate at any point during the reaction did not result in **$Mn_{10}W_4$-$P_8W_{48}$**, instead led to formation of unidentified yellow precipitate. The origin of the solitary $Na^+$ in the cluster is unclear.

### Single-crystal X-ray structure determination

The molecular and packing structure of **KLiMn-$Mn_{10}W_4$-$P_8W_{48}$** were determined by single-crystal X-ray diffraction (Figure 1-3). Compound **KLiMn-$Mn_{10}W_4$-$P_8W_{48}$** crystallizes in monoclinic symmetry in the space group *C2/c* with $Z = 4$. Polyanion **$Mn_{10}W_4$-$P_8W_{48}$** is composed of crown -shaped $\{P_8W_{48}\}$ in which an isopolytungstate anion $\{W_4O_{16}\}^{8-}$ is unprecedentedly entrapped exactly at the center of macrocycle, and is anchored in position by six $Mn^{II}$ centers grafted to the inner rim of the $\{P_8W_{48}\}$ POM (Figure 1). In addition, four $Mn^{II}$ centers have also been attached to the outer surface of the ring by coordination to oxido ligands from the $P_8W_{48}$ crown ring (Figure 2). Polyanion **$Mn_{10}W_4$-$P_8W_{48}$** is the first example where six $Mn^{II}$ centers have been incorporated in the inner rim of the superlacunary POM $\{P_8W_{48}\}$. The embedded isopolyanion is composed of four edge-shared $WO_6$ octahedra forming a planar butterfly topology. With respect to their coordination environment, these manganese anchors are of three types: only two of the six $Mn^{II}$ ions (Mn1) are linked to $\{P_8W_{48}\}$ by two Mn1–O(W) and two Mn1–O(P) bonds each, therefore, the four phosphate groups of $\{P_8W_{48}\}$ are not involved in the binding to the anionic isopolytungstate via Mn linkers. The rest of the coordination environment are filled by terminal oxygen atoms of two W centers in $(W_4O_{16})$ POM. Whereas, two $Mn^{II}$ ions (Mn2) each form two covalent Mn–O($W_{het}$), Mn–O($W_{iso}$) bonds and the four remaining octahedral coordination sites on each atom are occupied by $H_2O$.

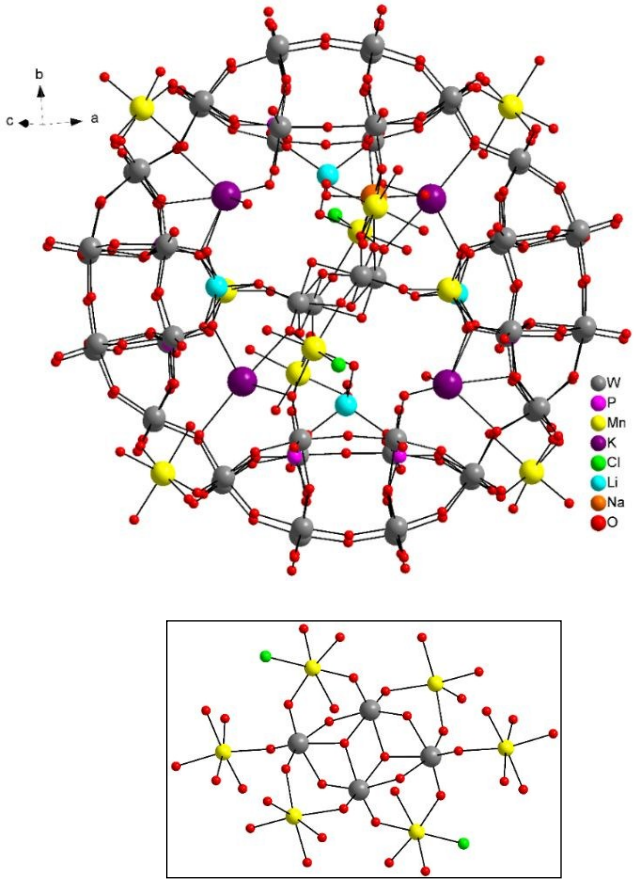


Fig. 1: Ball-and-stick representation. Above: Polyanion $[(P_8W_{48}O_{184})(W_4O_{16})K_{10}Li_4Mn_{10}Na(H_2O)_{50}Cl_2]^{15-}$ . Below: $(W_4O_{16})$ isopolyanion with $Mn^{II}$ anchors.

Two $Mn^{II}$ anchors (Mn3) each make link between two W atoms of the isopolyanion ($W_4O_{16}$) and one W atom of the crown-type heteropolyanion $\{P_8W_{48}\}$ ($(W_{iso})O_2$–Mn–$O(W_{het})$) through oxo ligands, remaining two coordination sphere is filled by the two aqua ligands and one chloro ligand. The Mn-O bond lengths are all in the range 2.087-2.315 Å, while Mn3-Cl1 is 2.365 Å. The oxidation states of the Mn cations were checked by Bond Valence Sum analysis,[46] and all were found to be $Mn^{II}$ (calculated values: Mn1 1.91, Mn2 2.03, Mn3 2.20, Mn4 2.03, Mn5A 2.10).

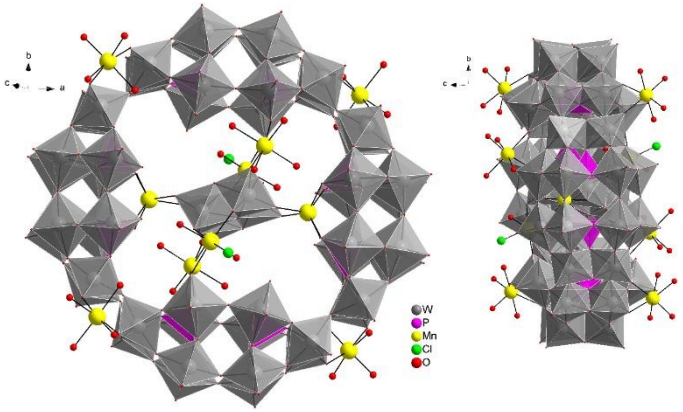


Fig. 2: Combined polyhedral/ball-and-stick representation. Front and side view of the structure of **$Mn_{10}W_4$-$P_8W_{48}$**. Alkali metal cations omitted for clarity.

The alkali metal cations ($4K^+$ and $4Li^+$) are also coordinated to the rim of the central cavity forming a ring of alternating $K^+$ and $Li^+$ centers. The four $K^+$ cations reside in the inner cavity of $\{P_8W_{48}\}$ at the vacant sites between neighboring $\{P_2W_{12}\}$ subunits. The 3D framework of this assembly is achieved via intramolecular Mn–O(W) bonding and linking potassium ions (Figure 3).

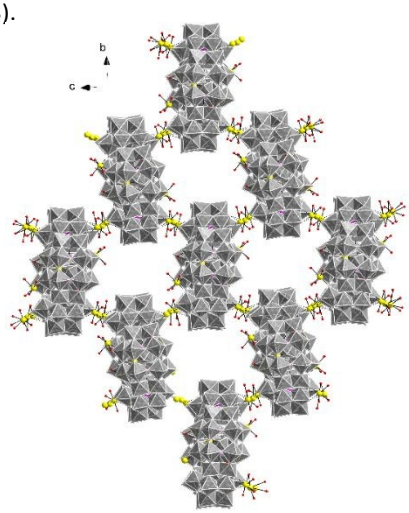

Fig. 3: Combined polyhedral/ball-and-stick representation of the crystal packing arrangement in **$Mn_{10}W_4$-$P_8W_{48}$**. Alkali metal cations omitted for clarity. $WO_6$ octahedra (gray), O (red), P (pink), Mn (yellow).

The $Na^+$ is only of half occupancy in the asymmetric unit, so there is on average one per cluster unit, though sodium ion was not added in the reaction mixture. To the best of our knowledge **$Mn_{10}W_4$-$P_8W_{48}$** is the first example of a wheel-shaped polyanion $\{P_8W_{48}\}$ that incorporates an isopolyoxotungstate anion.

## Experimental section

### General methods and materials

The POM ligand, $K_{28}Li_5[H_7P_8W_{48}O_{184}]\cdot 92\,H_2O$ $\{P_8W_{48}\}$ was synthesized according to the literature methods and was characterized by FTIR spectroscopy.[21] All reactions were carried out under aerobic conditions. All other reagents were purchased commercially and were used without further purification.

### Synthesis of $K_3Li_8Mn_2[(P_8W_{48}O_{184})(W_4O_{16})K_{10}Li_4Mn_{10}Na(H_2O)_{50}Cl_2]\cdot 62H_2O$ (KLiMn-$Mn_{10}W_4$-$P_8W_{48}$)

$K_{28}Li_5[H_7P_8W_{48}O_{184}]\cdot 92\,H_2O$ (0.37 g, 0.020 mmol) was dissolved in 15 mL of I M lithium chloride solution. Then $Mn(ClO_4)_2.6H_2O$ (0.15 g, 0.41 mmol) was added to this solution under stirring. The pH of the resultant turbid solution was raised to ca. 10 with 4 M LiOH. After stirring for 5 minutes, the pH was carefully adjusted to ca. 8 with HCL. The reaction mixture was then stirred and heated at 85 °C for one hour. Later the solution was filtered and left to slowly evaporate at room temperature, and pale yellow crystals were obtained after approximately three weeks. Yield 0,047g . IR (2% KBr pellet, $\nu/cm^{-1}$):1133 (wk), 1105 (wk), 1076 (wk), 1041(wk), 1015 (wk), 921 (shp), 786 (brd) 668 (brd). Elemental analysis (%) calc (found): K 3.11 (3.07), Li 0.51 (0.52), Na 0.15 (0.05), W 58.53 (58.30), P 1.52 (1.81), Mn 4.04 (4.05).

### X-ray crystallography

Data on single crystal of **KLiMn-$Mn_{10}W_4$-$P_8W_{48}$** was collected at 180 K using a Stoe IPDS II area detector diffractometer with graphite-monochromated Mo-K$\alpha$ radiation. Semi-empirical absorption corrections were applied using XPREP in SHELXTL.[41] Structure solution was by dual-space direct-methods (SHELXT)[42] followed by full-matrix least-squares refinement (SHELXL-2018)[43] within the Olex2 platform.[44] Anisotropic temperature factors were used for all ordered non H atoms, except $Li^+$ cations and some oxygens of lattice waters. The counter cations within or on the periphery of the cluster were ordered and could be refined anistropically with their coordinated waters. Further out from the clusters, other countercations and waters were badly disordered and could not be modeled; their contribution to the structure factors was calculated using SQUEEZE.[45]The overall formulation was based on analytical data, and this formula is that given in the cif. The oxidation numbers of the Mn cations were checked using Bond Valence Sum analysis.[46]

Further details of the crystal structures investigation may be obtained from FIZ Karlsruhe, 76344 Eggenstein-Leopoldshafen, Germany, https://www.ccdc.cam.ac.uk/structures/, on quoting the deposition number CSD-1922312.

Table 1: Crystal Data

| **Compound** | **KLiMn-$Mn_{10}W_4$-$P_8W_{48}$** |
|---|---|
| Formula | $Cl_2H_{224}K_{13}Li_{12}Mn_{12}NaO_{312}P_8W_{52}$ |
| Formula weight / g $mol^{-1}$ | 16370.49 |
| Crystal System | monoclinic |
| Space Group | C2/c |
| *a* / Å | 39.2947(14) |
| *c* / Å | 30.2573(6) |
| *U* / $Å^3$ | 27.7045(10) |
| Z | 4 |
| T / K | 180(2) |
| *F*(000) | 29264 |
| $D_c$ / g $cm^{-3}$ | 3.929 |
| □(Mo-K□) / $mm^{-1}$ | 22.436 |
| Data Measured | 95098 |
| Unique Data | 25538 |
| $R_{int}$ | 0.0748 |
| Data with I ≥ 2□(I) | 15912 |
| $wR_2$ (all data) | 0.1081 |
| *S* (all data) | 0.885 |
| $R_1$ [I≥2□(I)] | 0.0452 |
| Parameters/Restraints | 1616 / 20 |
| Biggest diff. peak/hole / eÅ$^{-3}$ | +2.32 / -2.66 |
| FIZ/CSD number | 1922312 |

### Powder X-ray diffraction (PXRD) analysis

Powder X-ray diffraction (PXRD) analysis was carried out on **KLiMn-$Mn_{10}W_4$-$P_8W_{48}$** to confirm the identity and phase purity of crystalline material. As shown in Fig 4 the experimental pattern is in consistent with the simulated one (on the basis of the single-crystal structure), which indicated the phase purity of the sample. The minor shift in the peaks reflects changes in the unit cell due to the fact single crystal measurement was carried out at 100 K, whereas, the PXRD data was collected at the room temperature. There might be some loss of lattice water molecules during PXRD measurement.

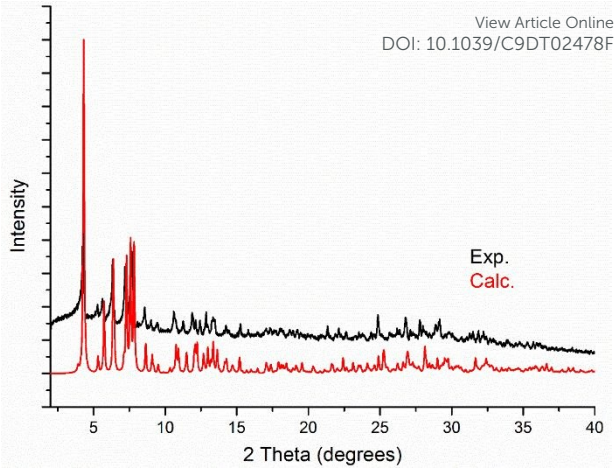


Fig. 4. Experimental diffraction powder pattern of **KLiMn-$Mn_{10}W_4$-$P_8W_{48}$** and calculated diffraction powder pattern from the single-crystal X-ray diffraction structure of **KLiMn-$Mn_{10}W_4$-$P_8W_{48}$.**

### Fourier-transform infrared (FTIR) spectroscopy

Infrared spectroscopy is another frequently employed analytical tool for the characterization of polyoxometalates due to its characteristic peaks in the in the region (1200-450 $cm^{-1}$) which is called the fingerprint region for the POM skeleton and result from stretch vibration frequency of the metal-oxygen. FTIR spectra were recorded on the precursor $\{P_8W_{48}\}$ and the isolated product **KLiMn-$Mn_{10}W_4$-$P_8W_{48}$** in order to further confirm the structural information and bulk purity. In the IR spectrum of $\{P_8W_{48}\}$, a set of bands in the range of 1135–400 $cm^{-1}$ are the characteristic bands of the $\{P_8W_{48}\}$ skeleton. The characteristic peaks at 1138, 1083, and 1015 $cm^{-1}$ are attributed to P–O vibrations of polyoxoanion precursor. The strong peak at 925 $cm^{-1}$ belongs to the stretching vibrations of the terminal W=O bonds. The characteristic peaks at 820–400 $cm^{-1}$ can be assigned to the W–O–W and W–O–P vibrations. The changes and splits observed in the stretching frequencies of the IR spectrum of **KLiMn-$Mn_{10}W_4$-$P_8W_{48}$** in comparison with superlacunary precursor $\{P_8W_{48}\}$ indicated the formation of new compound (Figure S1).

### Thermogravimetric analysis

In order to estimate the total content of the water molecules in bulk sample thermogravimetric analysis (TGA) was conducted. The TG curve of the compound **KLiMn-$Mn_{10}W_4$-$P_8W_{48}$** in the range of room temperature–950°C exhibit a two weight loss steps up to ca.550 °C. The total weight loss is ca. 12 % which correspond to the removal of the crystal waters (62) and the coordinated water molecules (50) (Figure S2). The overall elemental composition of the bulk material was also determined by complete elemental analysis.

### Electrochemical experiments

View Article Online
DOI: 10.1039/C9DT02475E



Pure water was obtained with a Milli-Q Intregral 5 purification set. All reagents were of high-purity grade and were used as purchased without further purification: $CH_3CO_2H$ (Glacial, Prolabo Normapur), $H_2SO_4$ (Sigma Aldrich), $Li_2SO_4.H_2O$ (Acros Organics) and $LiCH_3CO_2.2H_2O$ (Acros Organics). The composition of the various media was as follows: for pH 3.0, 0.5 M $Li_2SO_4$ + $H_2SO_4$ and for pH 5.0, 1.0 M $LiCH_3CO_2$ + $CH_3CO_2H$. The stability of the different compounds in solution was assessed by cyclic voltammetry.

Electrochemical data were obtained using an EG & G 273 A potentiostat driven by a PC with the M270 software. A one-compartment cell with a standard three-electrode configuration was used for cyclic voltammetry experiments. The reference electrode was a saturated calomel electrode (SCE) and the counter electrode platinum gauze of large surface area; both electrodes were separated from the bulk electrolyte solution via fritted compartments filled with the same electrolyte. The working electrodes were a 3 mm outer diameter EPG from Mersen, France. The pre-treatment of the first electrode before each experiment is adapted from a method described elsewhere.[47] Prior to each experiment, solutions were thoroughly de-aerated for at least 30 min with pure argon. A positive pressure of this gas was maintained during subsequent work. All cyclic voltammograms (CVs) were recorded at a scan rate of 10 mV $s^{-1}$ and potentials are quoted against SCE unless otherwise stated. The polyanion concentration was 0.07 mM. All experiments were performed at room temperature, which is controlled and fixed for the laboratory at 20°C. Results were very reproducible from one experiment to the other and slight variations observed over successive runs are rather attributed to the uncertainty associated with the detection limit of our equipment (potentiostat, hardware and software) and not to the working electrode pre-treatment nor to possible fluctuations in temperature.

**Electrochemistry**

As is often the case, the medium used for the synthesis is not the sole one in which the POM is stable, fortunately. The CVs recorded at pH 8 show badly defined waves and therefore present no real interest for the study. The media selected for the study (at pH 3 and 5) are usually more appropriate to obtain unambiguous electrochemical responses with POMs, rendering easier the comparison of the redox properties of species belonging to the same family.

The stability of **$Mn_{10}W_4$-$P_8W_{48}$** was assessed by cyclic voltammetry both at pH 3 and 5 upon recording several CVs at regular times for 6 hours. No major evolutions of the curves, which could be indicative of the decay of the POM in these media, were observed during this time span.

Therefore, in order to render the electrochemical features of the species **$Mn_{10}W_4$-$P_8W_{48}$** more obvious, we have carried out a comparative study with its parent compound {$P_8W_{48}$}.[21]The purpose was to reveal the influence of the $Mn^{II}$ centres present in the new species on its electrochemical behaviour. The comparison of the CVs of the two compounds recorded in the same experimental conditions, both at pH 3 and at pH 5, shows no marked differences as far as their shapes are concerned on the negative side of the potential scale (Figure S3). The reduction waves peak at almost the same potential values, namely at pH 3 (Table 2). On the positive side of the potential scale, the CV of **$Mn_{10}W_4$-$P_8W_{48}$** exhibits an oxidation wave attributed to the $Mn^{II}$ centres, which is also the case for the majority of POMs containing Mn centres.[30,48–53]The shape of this oxidation wave, as well as that of its associated reduction wave, clearly indicate the involvement of film adsorption and desorption phenomena taking place on the surface of the working electrode, probably made of manganese oxides.

Table 2. Values of the reduction, Ec, and oxidation, Ea, peak potentials (in V vs SCE), measured from the CVs recorded in the above-mentioned conditions, i.e.: working electrode: EPG; counter electrode: Pt wire; reference electrode: SCE; scan rate: 10 mV.$s^{-1}$, both at pH 3, 0.5 M $Li_2SO_4$ + $H_2SO_4$ and at pH 5, 1.0 M $LiCH_3CO_2$ + $CH_3CO_2H$.

| | | W | | | Mn | | | | |
|---|---|---|---|---|---|---|---|---|---|
| | | **$Ec_1$** | **$Ec_2$** | | **$Ec_1$** | **$Ec_2$** | | **$Ea_1$** | |
| **pH 3** | **$Mn_{10}W_4$-$P_8W_{48}$** | -0.51 | -0.64 | | -0.05 | 0.82 | | 1.07 | |
| | $P_8W_{48}$ | -0.52 | -0.65 | | | | | | |
| | | | | | | | | | |
| | | **Ec** | | | | **Ec** | | **$Ea_1$** | **$Ea_2$** |
| **pH 5** | **$Mn_{10}$-$P_8W_{48}$** | -0.91 | | | | 0.57 | | 0.82 | 1.36 |
| | $P_8W_{48}$ | -0.97 | | | | | | | |

At pH 3, and upon successive cycling, there is another reduction wave peaking at -0.05 V vs. SCE as from the second cycle onwards (Figure 5A, red curve), which is assigned to the reduction and concomitant desorption of some remnants of the layer of manganese oxides that may not have been totally eliminated at the reduction step at +0.82 V vs. SCE. The thickness of the film increases upon successive cycling (Figure 5B), but the application of sufficiently negative potentials (< -0.3 V vs. SCE) allows an almost total regeneration of the surface of the working electrode, and therefore of its previous electrochemical response. This behaviour has been analysed in more detail in a recent study using a quartz crystal microbalance and XPS spectroscopy.[50]

The formation of manganese oxides has already been observed and described for POMs possessing $Mn^{II}$ centres,[48,50,51,53] namely a species having the same structure as **$Mn_{10}W_4$-$P_8W_{48}$** but containing just 4 $Mn^{II}$ centres.[30] If all the $Mn^{II}$ centres were

removed from **$Mn_{10}W_4$-$P_8W_{48}$**, possibly as manganese oxides which would be deposited on the surface of the working electrode, the species remaining in solution would be **{$P_8W_{48}$}**, which is stable from pH 0 to 8.[21,54] The reduction and re-dissolution of these oxides may regenerate the parent compound, but the quantities of **$Mn_{10}W_4$-$P_8W_{48}$** involved under our experimental conditions are so small that no difference would be noticed in the CVs if the concentration happen to decrease slightly.

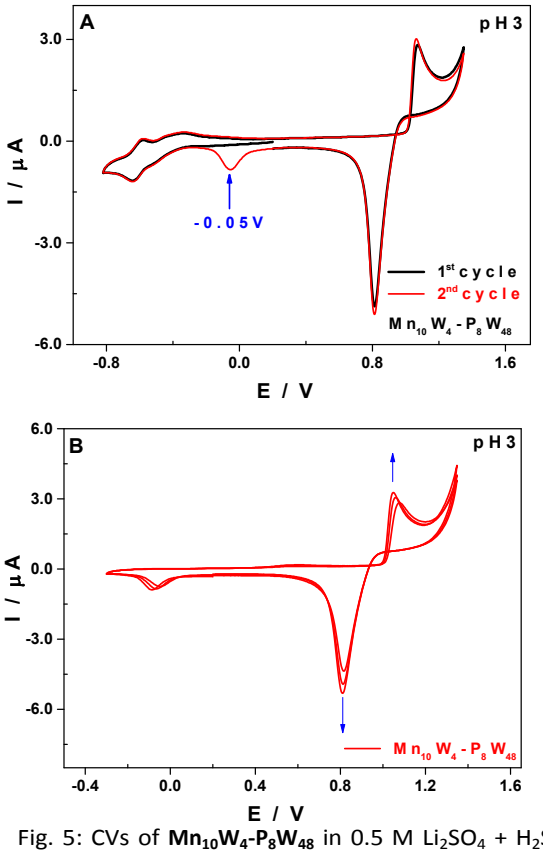


Fig. 5: CVs of **$Mn_{10}W_4$-$P_8W_{48}$** in 0.5 M $Li_2SO_4$ + $H_2SO_4$ / pH 3.0. POM concentration: 0.07 mM. (A) Potential range comprised between 1.35 V and -0.82 V. The scan was started at +0.2 V towards the negative potentials. (B) Potential range comprised between 1.35 V and -0.30 V. The scan was started at +0.2 V towards the positive potentials. Working electrode: EPG; counter electrode: Pt wire; reference electrode: SCE. Scan rate: 10 mV.$s^{-1}$.

At pH 5, other than the expected shift of the pH-dependent waves towards more negative potentials when compared to pH 3 (Table 2 and Figure S4), there are two points worth mentioning. First, the second re-dissolution step of the film of manganese oxides is no longer observed, the whole process taking place in a single reduction wave peaking at 0.57 V vs. SCE (Figure 6A).

Second, the general cathodic shift allows to explore another oxidation wave peaking at 1.36 V vs. SCE and being irreversible. This observation is in good agreement with other studies which have demonstrated that the $Mn^{II}$ centres could be oxidised beyond the oxidation state +IV and be involved in the electro-catalytic oxidation of water.[50,53] In this respect, the behaviour of the compound **$Mn_{10}W_4$-$P_8W_{48}$** is distinct from that of the homologous species possessing just four Mn centres, $Mn_4$-$P_8W_{48}$.[54] indeed, the oxidation peak potentials of the $Mn^{II}$ centre waves of the two compounds are very close, at pH 5: 0.82 V for **$Mn_{10}W_4$-$P_8W_{48}$** and 0.83 V for $Mn_4$-$P_8W_{48}$. No second oxidation wave has been described for the latter. The presence of this second wave in the case of **$Mn_{10}W_4$-$P_8W_{48}$** may be explained by a higher number of Mn centres in the POM and by their location in the molecular scaffold. As is often the case for Mn-containing POMs, the formation of a film made of manganese oxides on the surface of the working electrode renders tricky the determination by electrolysis of the number of electrons involved in the oxidation steps. As a consequence, it is not obvious to confirm the number of Mn centres present in the POM using electrochemical methods.

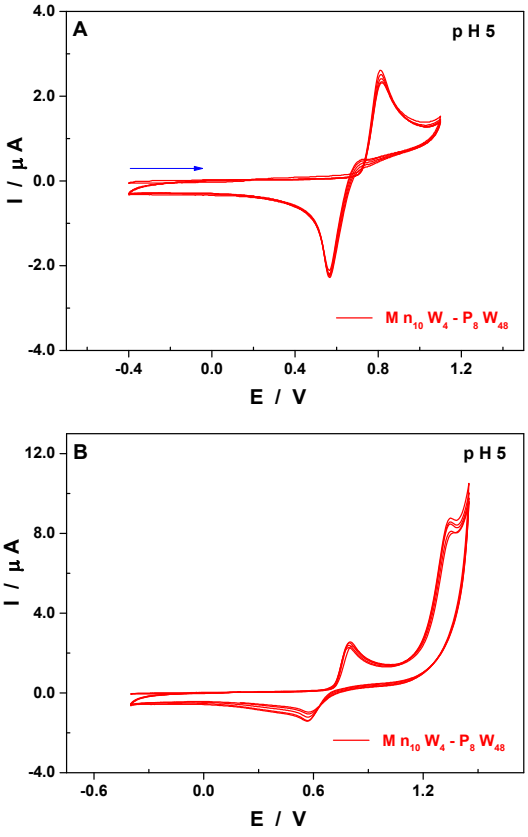


Fig. 6: CVs of **$Mn_{10}W_4$-$P_8W_{48}$** in 1.0 M $LiCH_3CO_2$ + $CH_3CO_2H$ / pH 5.0. POM concentration: 0.07 mM. (A) Potential range comprised between 1.10 V and -0.40 V. The scan was started at +0.2 V towards the negative potentials. (B) Potential range comprised between 1.45 V and -0.40 V. The scan was started at +0.2 V towards the positive potentials. Working electrode: EPG; counter electrode: Pt wire; reference electrode: SCE. Scan rate: 10 mV.$s^{-1}$.

DOI: 10.1039/C9DT02478F

## Conclusions

In summary, we have demonstrated here that an unprecedented isopolyanion ($W_4O_{16}$) can be embedded within cavity of archetypal superlacunary POM {$P_8W_{48}$}by direct reaction of $Mn^{II}$ ions with $[H_7P_8W_{48}O_{184}]^{33-}$ in basic medium using simple, one-pot procedure. The obtained POM has been characterized by single crystal X-ray crystallography, powder X-ray diffraction (PXRD), Fourier-transform infrared (FTIR) spectroscopy, elemental analysis and thermogravimetric analysis. Electrochemical studies performed on **$Mn_{10}W_4$-$P_8W_{48}$** in aqueous media confirmed the presence of Mn centers and showed their influence on its redox behavior. Single X-ray diffraction data revealed that polyanion **1** has been isolated in the solid state as the hydrated mixed potassium/lithium/manganese salt **KLiMn-$Mn_{10}W_4$-$P_8W_{48}$**. The ($W_4O_{16}$) unit is held in the central cavity of the {$P_8W_{48}$} by six $Mn^{II}$ ions as linkers/anchors. Polyanion **$Mn_{10}W_4$-$P_8W_{48}$** is the first example where an isopolyanion has been inserted within {$P_8W_{48}$} cavity, further, the largest number of $Mn^{II}$ centers have been incorporated in the inner cavity of the macrocyclic ligand. Currently we are investigating the possibility of encapsulation of other transition metal assemblies within the cavity of cylic {$P_8W_{48}$} POM. The host-guest architectures based on macrocyclic ring {$P_8W_{48}$} allows for the construction of various structures which might display an interesting set of properties in various fields such as ion exchange, gas storage, catalysis and medicine.

## Acknowledgements

M. I. thanks Prof. Annie. K. Powell for her continuous support and guidance. M.I. acknowledges support by the Helmholtz society through program Science and Technology of Nanosystems (STN). M.I. also thanks the University of Balochistan, Quetta, Pakistan for allowing her to pursue her Ph.D and postdoctoral work at Jacobs University and KIT, respectively. We also thank Sven Stahl and Dr. Thomas Bergfeldt for performing TGA measurements and elemental analysis respectively. This work was partially carried out with the support of the Karlsruhe Nano Micro Facility (KNMF), a Helmholtz research infrastructure at Karlsruhe Institute of Technology. We also thank the Université Paris-Sud and the CNRS for financial support.

## Notes and references

1 D. L. Long, R. Tsunashima and L. Cronin, *Angew. Chem., Int. Ed.*, 2010, 49, 1736–1758.

2 M. T. Pope, *Heteropoly and Isopoly Oxometalates*, Springer, Berlin, 1983.

3 C. Vonci, M, Boskovic, *Aust. J. Chem.*, 2014, 67, 1542–1552.

4 M. Ibrahim, Y. Lan, B. S. Bassil, Y. Xiang, A. Suchopar, A. K. Powell and U. Kortz, *Angew. Chem., Int. Ed*, 2011, 50, 4708–4711.

5 X. Han, Y. Li, Z. Zhang, H. Tan, Y. Lu and E. Wang, *J. Am. Chem. Soc.*, 2015, 137, 5486–5493.

6 O. Oms, A. Dolbecq and P. Mialane, *Chem. Soc. Rev.*, 2012, 41, 7497–7536.

7 A. Haider, M. Ibrahim, B. S. Bassil, A. M. Carey, A. N. Viet, X. Xing, W. W. Ayass, J. F. Miñambres, R. Liu, G. Zhang, B. Keita, V. Mereacre, A. K. Powell, K. Balinski, A. T. N'Diaye, K. Küpper, H.-Y. Chen, U. Stimming and U. Kortz, *Inorg. Chem.*, 2016, 55, 2755–2764.

8 M. Ibrahim, A. Haider, Y. Xiang, B. S. Bassil, A. M. Carey, L. Rullik, G. B. Jameson, F. Doungmene, I. M. Mbomekallé, P. De Oliveira, V. Mereacre, G. E. Kostakis, A. K. Powell and U. Kortz, *Inorg. Chem.,* 2015, 54, 6136–6146.

9 B. S. Bassil, M. Ibrahim, R. Al-Oweini, M. Asano, Z. Wang, J. Van Tol, N. S. Dalal, K. Y. Choi, R. Ngo Biboum, B. Keita, L. Nadjo and U. Kortz, *Angew. Chem., Int. Ed,* 2011, 50, 5961–5964.

10 M. Ibrahim, S. S. Mal, B. S. Bassil, A. Banerjee and U. Kortz, *Inorg. Chem.*, 2011, 50, 956–960.

11 M. Ibrahim, B. Bassil and U. Kortz, *Inorganics*, 2015, 3, 267–278.

12 C. M. Granadeiro, B. De Castro, S. S. Balula and L. Cunha-Silva, *Polyhedron*, 2013, 52, 10–24.

13 B. S. Bassil, M. H. Dickman, I. Römer, B. Von Der Kammer and U. Kortz, *Angew. Chem., Int. Ed.*, 2007, 46, 6192–6195.

14 U. Kortz, A. Müller, J. van Slageren, J. Schnack, N. S. Dalal and M. Dressel, *Coord. Chem. Rev.*, 2009, 253, 2315–2327.

15 J. Zhao, Y. Li, L. Chen and G. Yang, *Chem. Comm.*, 2016, 52, 4418–4445.

16 B. S. Bassil and U. Kortz, *ZAAC.,* 2010, 636, 2222–2231.

17 S. Reinoso, *Dalton Trans.*, 2011, 40, 6610–6615.

18 S. Reinoso, J. R. Galán-Mascarós and L. Lezama, *Inorg. Chem.*, 2011, 50, 9587–9593.

19 M. Ibrahim, V. Mereacre, N. Leblanc, W. Wernsdorfer, C. E. Anson and A. K. Powell, *Angew. Chem., Int. Ed.,* 2015, 54, 15574–15578.

20 T. Yu, H. Ma, C. Zhang, H. Pang, S. Li and H. Liu, *Dalton Trans.*, 2013, 42, 16328–16333.

21 R. Contant and A. Teze, *Inorg. Chem.*, 1985, 24, 4610–4614.

22 S. S. Mal and U. Kortz, *Angew. Chem., Int. Ed.*, 2005, 3, 3777–3780.

23 C. Pichon, P. Mialane, A. Dolbecq, J. Marrot, E. Rivière, B. Keita, L. Nadjo and F. Sécheresse, *Inorg. Chem.* 2007, 46, 5292–5301.

24 S. S. Mal, B. S. Bassil, M. Ibrahim, S. Nellutla, J. Van Tol, N. S. Dalal, J. a. Fernández, X. López, J. M. Poblet, R. N. Biboum, B. Keita and U. Kortz, *Inorg. Chem.*, 2009, 48, 11636–11645.

25 A. Müller, M. T. Pope, A. M. Todea, H. Bögge, J. Van Slageren, M. Dressel, P. Gouzerh, R. Thouvenot, B. Tsukerblat and A. Bell, *Angew. Chem., Int. Ed.*, 2007, 46, 4477–4480.

26 S. S. Mal, M. H. Dickman, U. Kortz, A. M. Todea, A. Merca, H. Bögge, T. Glaser, A. Müller, S. Nellutla, N. Kaur, J. Van Tol, N. S. Dalal, B. Keita and L. Nadjo, *Chem. Eur.J.*, 2008, 14, 1186–1195.

27 V. S. Korenev, S. Floquet, J. Marrot, M. Haouas, I. M.

Mbomekallé, F. Taulelle, M. N. Sokolov, V. P. Fedin and E. Cadot, *Inorg. Chem.*, 2012, 51, 2349–2358.

28 N. V. Izarova, L. Klaß, P. De Oliveira, I. M. Mbomekalle, V. Peters, F. Haarmann and P. Kögerler, *Dalton Trans.*, 2015, 44, 19200–19206.

29 X. Yi, N. V. Izarova and P. Kögerler, *Inorg. Chem.,* 2017, 56, 13822–13828.

30 B. S. Bassil, M. Ibrahim, S. S. Mal, A. Suchopar, R. N. Biboum, B. Keita, L. Nadjo, S. Nellutla, J. Van Tol, N. S. Dalal and U. Kortz, *Inorg. Chem.*, 2010, 49, 4949–4959.

31 S. S. Mal, N. H. Nsouli, M. H. Dickman and U. Kortz, *Dalton Trans.,* 2007, 186, 2627-2630.

32 M. Zimmermann, N. Belai, R. J. Butcher, M. T. Pope, E. V. Chubarova, M. H. Dickman and U. Kortz, *Inorg. Chem.*, 2007, 46, 1737–1740.

33 K. Y. Wang, S. Zhang, D. Ding, T. Ma, U. Kortz and C. Wang, *Eur. J. Inorg. Chem.,*2019, 2019, 512–516.

34 I. M. Mbomekallé, B. S. Bassil, A. Suchopar, B. Keita, L. Nadjo, M. Ammam, M. Haouas, F. Taulelle and U. Kortz, *J. Clust. Sci.* 2014, 25, 277–285.

35 H. N. Miras, L. Vilà-Nadal and L. Cronin, *Chem. Soc. Rev.,* 2014, 43, 5679–5699.

36 S. G. Mitchell, D. Gabb, C. Ritchie, N. Hazel, D. L. Long and L. Cronin, *CrystEngComm*., 2009, 11, 36–39.

37 T. Boyd, S. G. Mitchell, D. Gabb, D. Long, Y. Song and L. Cronin, *J. Am. Chem. Soc*, 2017, 139, 5930–5938.

38 S. G. Mitchell, C. Streb, H. N. Miras, T. Boyd, D. L. Long and L. Cronin, *Nat. Chem.,* 2010, 2, 308–312.

39 P. Yang, M. Alsufyani, A. H. Emwas, C. Chen and N. M. Khashab, *Angew. Chem., Int. Ed.*, 2018, 57, 13046–13051.

40 A. Müller, S. Q. N. Shah, H. Bögge, M. Schmidtmann, *Nature*, 1999, 397, 48–50.

41 G. M. Sheldrick, *Acta Cryst*, 2015, A71, 3–8.

42 G. M. Sheldrick, *Acta Cryst*, 2015, 71, 3–8.

43 G.M. Sheldrick, *Acta Cryst.*, 2015, C71, 3–8.

44 H. P. O.V. Dolomanov, L.J. Bourhis, R.J. Gildea, J.A.K. Howard, *J. Appl. Cryst.*, 2009, 42, 339–341.

45 A.L. Spek, *Acta Cryst.*, 2015, C71, 9–18.

46 W. Liu and H. H. Thorp, *Inorg. Chem*, 1993, 32, 4102–4105.

47 N. Vilà, P. a. Aparicio, F. Sécheresse, J. M. Poblet, X. López and I. M. Mbomekallé, *Inorg. Chem.* 2012, 51, 6129–6138.

48 I. M. Mbomekalle, B. Keita, L. Nadjo, P. Berthet, W. a. Neiwert, C. L. Hill, M. D. Ritorto and T. M. Anderson, *J. Chem.Soc. Dalton Trans.*, 2003, 3, 2646–2650.

49 M. Lebrini, I. M. Mbomekallé, A. Dolbecq, J. Marrot, P. Berthet, J. Ntienoue, F. Sécheresse, J. Vigneron and A. Etcheberry, *Inorg. Chem.,* 2011, 50, 6437–6448.

50 A.-L. Teillout, P. de Oliveira, J. Marrot, R. Howell, N. Vilà, A. Walcarius and I. Mbomekallé, *Inorganics*, 2019, 7, 15.

51 J. Friedl, R. Al-Oweini, M. Herpich, B. Keita, U. Kortz and U. Stimming, *Electrochimica Acta*, 2014, 141, 357–366.

52 R. Al-Oweini, B. S. Bassil, J. Friedl, V. Kottisch, M. Ibrahim, M. Asano, B. Keita, G. Novitchi, Y. Lan, A. Powell, U. Stimming and U. Kortz, *Inorg. Chem.,* 2014, 53, 5663–5673.

53 B. Keita, P. Mialane, F. Sécheresse, P. de Oliveira and L. Nadjo, *Electrochem. Commun.*, 2007, 9, 164–172.

54 B. Keita, Y. W. Lu, L. Nadjo and R. Contant, Electrochem. Commun. 2000, 2, 720-726.